Heliyon 10 (2024) e30708

Contents lists available at ScienceDirect

Heliyon

journal homepage: www.cell.com/heliyon

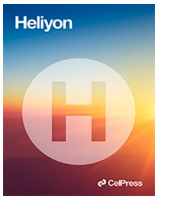

Research article

Chronotherapy involving rosiglitazone regulates the phenotypic switch of vascular smooth muscle cells by shifting the phase of TNF-α rhythm through triglyceride accumulation in macrophages

Yu Tian [a,b,1], Xuanyu Luan [c,1], Kui Yang [b,*]

[a] School of Pharmacy, Wannan Medical College, Wuhu, Anhui, 241001. PR China
[b] Department of Pharmacy, Yijishan Hospital of Wannan Medical College, Wuhu, Anhui, 241001, PR China
[c] Department of Metabolism, Digestion and Reproduction, Faculty of Medicine, Imperial College London, London, United Kingdom

ARTICLE INFO

Keywords:
Chronotherapy
PPARγ agonists
Macrophages
VSMCs phenotype switch
Clock gene
Lipid metabolism

ABSTRACT

Objectives: Vascular diseases are often caused by the interaction between macrophages and vascular smooth muscle cells (VSMCs). This study aims to elucidate whether chronotherapy with rosiglitazone (RSG) can regulate the secretion rhythm of macrophages, thereby controlling the phenotypic switch of VSMCs and clarifying the potential molecular mechanisms, providing a chronotherapeutic approach for the treatment of vascular diseases.

Methods: RAW264.7 cells and A7r5 cells were synchronized via a 50 % FBS treatment. M1-type macrophages were induced through Lipopolysaccharide (LPS) exposure. Additionally, siRNA and plasmids targeting PPARγ were transfected into macrophages. The assessment encompassed cell viability, migration, inflammatory factor levels, lipid metabolites, clock gene expression, and relative protein expression.

Results: We revealed that, in alignment with core clock genes Bmal1 and CLOCK, RSG administration at ZT2 advanced the phase of TNF-α release rhythm, while ZT12 administration shifted it backward. Incubation with TNF-α at ZT2 significantly promoted the phenotype switch of VSMCs. This effect diminished when incubated at ZT12, implicating the involvement of the clock-MAPK pathway in VSMCs. Furthermore, RSG administration at ZT2 advanced the phases of PPARγ and Bmal1 genes, whereas ZT12 administration shifted them backward. Additionally, PPARγ overexpression significantly induced triglyceride (TG) accumulation in macrophages. Exogenous TG upregulated Bmal1 and CLOCK gene expression in macrophages and significantly increased TNF-α release.

Conclusion: Chronotherapy involving RSG induces TG accumulation within macrophages, resulting in alterations in circadian gene rhythms. These changes, in turn, modulate the phase of rhythmic TNF-α release and play a regulatory role in VSMCs phenotype switch. Our study establishes a theoretical foundation for chronotherapy of PPARγ agonists.

* Corresponding author.
E-mail address: ykui15556689670@163.com (K. Yang).
[1] These authors contributed equally to this paper.

https://doi.org/10.1016/j.heliyon.2024.e30708
Received 14 December 2023; Received in revised form 2 May 2024; Accepted 2 May 2024
Available online 16 May 2024

1. Introduction

Vascular smooth muscle cells (VSMCs) drive cardiovascular disease (CVD) via phenotype switch [1,2]. It is widely recognized that controlling the phenotypic transition of VSMCs is beneficial for treating CVDs [3,4]. In response to stress or vascular injury, contractile VSMCs can switch to a less differentiated state (synthetic phenotype) to acquire the proliferative, migratory, and synthetic capabilities for tissue reparation [5,6]. Macrophages may exert control over the phenotype switch of VSMCs through intracellular communication via the release of inflammatory factors. Once infiltrating the intima, monocyte-derived macrophages can polarize to the M1 state, secreting various cytokines and chemokines, such as tumor necrosis factor-alpha (TNF-α) and interleukin 6 (IL-6), to further activate the phenotypic switch of VSMCs [7,8]. Therefore, targeting macrophages may represent an effective approach to regulating the phenotypic switch of VSMCs.

The clock system regulates the functioning of macrophages. At the molecular level, the clock system consists of a set of transcriptional-translational feedback loops (TTFLs) comprising various clock genes and clock proteins [9]. In essence, the primary TTFL is governed by the basic helix-loop-helix ARNT-like 1 (Bmal1) and CLOCK heterodimers, which promote the transcription of target clock-controlled genes like periods (Per1-3) and cryptochromes (Cry1-2). Conversely, the Per and Cry proteins can form heterodimers that translocate to the nucleus, where they inhibit their transcription by interacting with the BMAL1 and CLOCK complex, creating a negative feedback loop [10]. Notably, macrophages also possess a molecular clock, with more than 8 % of all genes displaying circadian rhythms. Research has shown that the inflammatory cytokines released by macrophages follow a circadian rhythm [11]. However, whether the circadian rhythm of inflammatory cytokines released by macrophages regulates the phenotypic switch of VSMCs remains largely unexplored.

Chronotherapy is a medical approach focused on synchronizing medical treatments, especially medications and interventions, with the body's natural circadian rhythms. It has proven effective in regulating the circadian rhythm of inflammatory cytokines [12]. Similarly, targeting the clock system is an integral component of chronotherapy. However, the precise methodology for implementing this treatment approach remains controversial. Peroxisome proliferator-activated receptor gamma (PPARγ) is among the ligand-dependent nuclear hormone receptors known to impact lipid metabolism and adipose function [13]. Furthermore, as a transcription factor, research has shown that PPARγ can activate the expression of BMAL1 by binding to PPAR response elements (PPRE) in the promoter region of BMAL1[14]. Consequently, targeting the clock system in macrophages to regulate the rhythmic release of inflammatory cytokines, ultimately influencing the phenotypic switch of VSMCs through the activation of PPARγ, appears to be a feasible approach. Nonetheless, the precise signaling cascade between PPARγ and BMAL1 in macrophages remains largely unexplored.

In this study, we utilized the PPARγ agonist rosiglitazone (RSG) to treat LPS-induced M1 macrophages at different time points, monitoring the rhythmic release of inflammatory cytokines from these macrophages. Additionally, we evaluated the impact of these rhythmic changes in inflammatory cytokine release on the phenotypic transition of VSMCs. On the molecular level, we delved into how the activation of PPARγ within macrophages triggers alterations in the endogenous circadian gene rhythms. Our findings revealed that PPARγ activation within macrophages prompts the accumulation of triglycerides (TG), leading to shifts in the circadian gene rhythms within these macrophages. These alterations subsequently influence the timing of rhythmic inflammatory cytokine release and contribute to the regulation of VSMC phenotypic changes. Our study establishes a conceptual framework for timing-based treatments of vascular diseases attributed to VSMCs, leveraging the potential of PPARγ agonists.

2. Materials and methods

2.1. Reagents

RSG was purchased from MK Bio Science Co., Inc. (Shanghai, China). Lipopolysaccharide (LPS) was a gift from AbMole (Beijing, China). Recombinant protein TNF-α was obtained from Sino Biological (Beijing, China). Palmitic acid (PAL) and TG were purchased from MedChemExpress (MCE, Shanghai, China).

2.2. Mouse serum obtained and cell culture

A total of 5 C57BL/6J mice were procured from Tianqin Biology Co., Ltd (Hunan, China). This animal experiment received approval from the Ethics Committee of Wannan Medical College (Ethics Approval Number: WNMC-AWE-2023332). All procedures strictly adhered to regulatory guidelines and standards, following the principles of the declaration of Helsinki. Before obtaining the necessary animal samples, we uphold the highest ethical standards and make every effort to minimize harm and suffering to the animals. RAW264.7 cells (macrophages) and A7r5 cells (VSMCs) were obtained from The Procell Life Science & Technology (Wuhan, China). These cells were cultured in DMEM/F12 (1:1) medium (Gibco, CA, USA) supplemented with 10 % fetal bovine serum (FBS) (Gibco, CA, USA) and 1 % penicillin-streptomycin (Beyotime, Shanghai, China) for routine maintenance. The cells were incubated at 37 °C in a humidified atmosphere with 5 % CO_2. The growth medium was replaced every 2–3 days, and the cells were subcultured onto porous dishes or multi-well plates at a 1:3 ratio when they reached 80 % confluence.

2.3. Circadian rhythm synchronization

To synchronize the circadian rhythm of the cells, the cell culture medium was substituted with DMEM containing 50 % FBS. When the VSMCs began to incubate with 50 % serum shocking, this time point was recorded as Zeitgeber time 0 (ZT 0). After 2 hours of

cultivation with 50 % serum shocking, it is recorded as ZT2. Then, after washing three times with PBS (Gibco, CA, USA), the cells can be processed. This procedure induces alterations in the circadian rhythms of affected cells. The expression of clock genes in VSMCs needs to be detected within a 35-hour to confirm whether circadian oscillations have been induced. We have previously validated that a 2-hour 50 % FBS incubation results in VSMCs exhibiting a stable circadian rhythm in our previous study [15].

2.4. Western blot

VSMCs were lysed with cold protein lysis buffer (RIPA) (Beyotime, Shanghai, China) supplemented with phenylmethanesulfonyl fluoride (PMSF) (Beyotime, Shanghai, China) and protease inhibitor mixture (Beyotime, Shanghai, China) in DMSO. After obtaining the supernatant, protein concentration was quantified using the BCA method (Beyotime, Shanghai, China). Subsequently, 50 μg of protein was subjected to electrophoresis on an 8–10 % SDS polyacrylamide gel and subsequently transferred onto nitrocellulose membranes (NC, Millipore, USA) in ice water for 75 min (300 mA). Following blocking with 10 % skim milk, the membranes were incubated overnight at 4 °C with primary antibodies. After thorough 3 times washing with TBST (Servicebio, Wuhan, China), the membranes subsequently incubated with HRP-conjugated goat anti-rabbit IgG or anti-mouse IgG (Supplement Table 1) at room temperature for 1 hour, Immunofluorescence signals were detected using the high-sensitivity Tanon 5200 system (BioTanon, Shanghai, China). The expression levels of relative phosphorylated proteins were normalized to unphosphorylated proteins. The expression levels of other proteins in this study were quantified and normalized to GAPDH expression. The standardization process was completed using image J.

2.5. Real-time quantitative polymerase chain reaction (qPCR)

The total RNA from each sample was isolated using Trizol reagent (TIANGEN, Beijing, China) following the manufacturer's instructions. Equal amounts of RNA (0.5 μg) from each sample were employed for cDNA synthesis, which was carried out using the FastKing RT Kit (With gDNase) designed for qPCR (TIANGEN, Beijing, China). Real-time quantitative PCR was performed using SuperReal PreMix Plus (SYBR Green) (TIANGEN, Beijing, China). The primer sequences can be found in Supplement Table 2. All primers were purchased from Generary Biotech Co., Ltd. (Shanghai, China). To determine the relative expression of Clock-related mRNAs, we calculated it based on the comparative quantification (Cq) obtained at the conclusion of each run. The relative quantification of gene expression was reported as a relative quantity in relation to the control value using the $2^{-\Delta\Delta Ct}$ method. GAPDH served as an internal control for each sample.

2.6. Small interfering RNA (siRNA) transfection

For PPARγ knockdown, RAW264.7 cells were seeded in six-well plates at an initial density of 10^5 cells/mL one day before transfection to establish a monolayer. When the cells reached 30–40 % confluence, they were washed and re-cultured in fresh medium without antibiotics. Transfection was performed individually using siRNA-PPARγ (100 nM) or scramble (NC) siRNA (100 nM) along with lipofectamine 3000 (Invitrogen, Shanghai, China), following the manufacturer's instructions. All siRNAs were obtained from Generary Biotech Co., Ltd. (Shanghai, China). To confirm the efficiency of PPARγ knockdown, three different siRNAs were utilized (Supplement Table 3). Following a 6-h incubation, the culture medium was replaced with medium containing 10 % serum and antibiotics. After 48 hours of incubation, the transfected RAW264.7 cells were harvested. Total RNA was extracted, and the transfection efficiency was validated through qPCR. The most effective inhibition of PPARγ was achieved using the target sequences CAATCAGGATGCACTTTCA for the PPARγ siRNA.

2.7. Plasmid transfection

For PPARγ overexpression, the plasmids PPARγ were purchased from Generary Biotech (Shanghai, China). The plasmid PPARγ (100 nM) was transfected with plasmids diluted using Lipofectamine 3000 according to the manufacturer's protocol. The transfection efficiency was verified by qPCR.

2.8. Cell viability assay

MTT (4,5 dimethyl-2-yl 2,5-diphenyl tetrazolium bromide) assay (Macklin Biochemical Co., Ltd., Shanghai, China) was employed to measure cell viability. The VSMCs were seeded in 96-well plates overnight and then VSMCs began incubation with 50 % serum for 2 hours in order to synchronization. After 3 times wash with PBS, TNF-α (0, 25, 50, 100, 200 ng/ml) was added at ZT2, ZT7, ZT12, ZT17 and ZT22 for 24 hours, respectively. After VSMCs were incubated with 5 mg/ml MTT at 37 °C for 4 hours. The medium was abandoned and 100 μl of dimethyl sulfoxide (DMSO) was added to each well and vibrated at low speed for 10 min. The absorbance was detected at 490 nm using a microplate reader (Bio-rad, Mekawa, Japan).

2.9. Cell proliferation assay

To identify VSMCs proliferation, the immunofluorescence staining was performed by using Ki-67, a marker for proliferating cells. The Ki-67 cell proliferation assay kit (Immunofluorescence, Green, Mouse Monoclonal Antibody) was purchased from Beyotime

Biotechnology (Shanghai, China). VSMCs were seeded in 96-well plates overnight, and when VSMCs began incubation with 50 % serum for 2 hours in order to synchronization. Then TNF-α (0, 25, 50, 100, 200 ng/ml) was added at ZT2 and ZT2 for 24 hours, respectively. VSMCs in 96-well plates were permeabilized with fixative solution for 10 min, then blotted out and washed, then blocked with immunostaining blocking solution for 20 min, and then incubated with primary anti-Ki-67 mouse monoclonal antibody at 4 °C overnight. The next day, after the primary antibody was aspirated and washed, the secondary antibody was added and incubated for an additional hour at room temperature. The nuclei were stained with DAPI. Photographs were taken under a fluorescence microscope (Zeiss, Germany). The number of Ki-67-positive cells was randomly counted in five different areas. The ki-67 labeling index was calculated by the ratio of Ki-67-positive VSMCs to the total number of VSMCs. The mean ki-67 labeling index was then obtained for each group.

2.10. Transwell assay

Transwell was performed to assess the vertical migration capability of VSMCs. For these studies, standard 24-well transwell inserts with a FluoroBlok PET membrane (Corning, Inc.) (8-mm pore size), were used. Briefly, VSMCs (4×10^4 cells/well) were seeded in serum-free medium in the upper chamber. And DMEM supplemented with 10 % FBS was added to the lower chamber. After cell synchronization, TNF-α (0, 25, 50, 100, 200 ng/ml) was added to ZT2 and ZT12 in the upper chamber, respectively. After incubating for 24 hours, the invaded cells in lower chamber were fixed using 4 % paraformaldehyde (Macklin, China), and the staining of these cells was performed using crystal violet (Servicebor, China) for 20 min. The count of invaded cells was conducted in five randomly chosen fields using a light microscope (Zeiss, Germany).

2.11. Scratch test

VSMCs were cultured in 6-well plates at a density of 5×10^5 cells/well. When the cell confluence reached approximately 90 %, a 10 μl pipette tip was used to create vertical scratches in the cell monolayer. Any detached cells were removed by washing the wells 3 times with PBS. During cell synchronization, mitomycin (1ug/ml) were added at ZT1 and treat for 1 hour. After 3 times wash with PBS, TNF-α (0, 25, 50, 100, 200 ng/ml) was added to ZT2 and ZT12 for 24 hours, respectively. Subsequently, the medium was replaced with fresh medium containing 2 % FBS, and the intercellular gap was observed under a low-magnification phase-contrast microscope (Olympus MK, Tokyo, Japan). After 24 hours of incubation, images of the cells in the same field were captured to assess changes in the width of the scratch. The migration rate was calculated using the formula: Migration capacity = initial scratch width/scratch width at 24 hours. Each experiment was repeated three times for validation.

2.12. Enzyme-linked immunosorbent assay (ELISA) and Biochemical analysis

RAW264.7 cells were seeded in 6-well plates overnight and synchronized. Then, ZT2 was followed by LPS (100 ng/ml) to induce M1 macrophages to release inflammatory cytokines, and ZT2 and ZT12 were supplemented with RSG (20 μmol), respectively. Cells were divided into four groups: control group, LPS group, LPS + ZT2 RSG group, and LPS + ZT12 RSG group. At ZT3, the first sampling was performed. We then ensured that consecutive samples were collected every 4 h for the next 35 h, and these time points were recorded as ZT7, ZT11, ZT15, ZT19, ZT23, ZT27, ZT31, and ZT35. Supernatants were collected for further analysis, and the levels of TNF-α, IL-6, and IL-1β in RAW264.7 cells were assessed using ELISA kits from Spbio (Wuhan, China) following the manufacturer's instructions.

In addition, RAW264.7 cells were evenly distributed in multiple 6-well culture plates overnight. After adding 10 % concentration mouse serum (MS) to macrophages, the macrophages were transfected with plasmid containing PPARγ gene sequence (100 nmol) to over-expression PPARγ (PPARγ-OE). Thus, cells were divided into 4 groups: Control, Control+10 % MS, Control+10 % MS + NC, Control+10 % MS + PPARγ-OE. After 48 hours, the supernatant samples were collected, and the expression levels of PAL, linoleic acid (LA), and diacylglycerol (DAG) in the cells were detected by ELISA kit of Spbio (Wuhan, China). Total protein concentration was determined using the BCA Protein Assay kit. TG and total cholesterol levels in cell samples were determined using biochemical kits from Jiancheng BioEngineering Institute (Nanjing, China). Optical density (OD) values at 450 nm were read using an iMark microplate reader (Bio-rad, Mekawa, Japan). In addition, all measurements were performed in duplicate three times.

2.13. Co-culture

A co-culture system was established using Transwell (Corning, USA, 3412, 24-well plates, 0.4 μm) chambers. VSMCs were seeded in the bottom of 24-well plates under sterile conditions with 10 % FBS. RAW264.7 cells were seeded in to the upper chamber also containing 10 % FBS. After the two kinds of cells adhered to the wall and grew, the original medium was removed, and the DMEM medium was added again to establish a co-culture system. There was no direct cell connection between the two cells, and RAW264.7 mainly affected VSMCs through the chamber membrane by secreting factors. VSMCs and co-cultures with untreated macrophages served as controls. After RAW264.7 cells began incubation with 50 % serum for 2 h in order to synchronization, addition of LPS (100 ng/ml) to the upper chamber at ZT2 time point. And the rosiglitazone (20 μmol) was added into upper chamber at ZT2 and ZT12, respectively. TNF-α neutralizing antibody (Sigma-Aldrich, USA) was added at a concentration of 1 μg/ml to inhibit TNF-α′s function. Cells were co-cultured for 24 h, and crystal violet staining is used to assess the quantity of cells in the lower chamber.

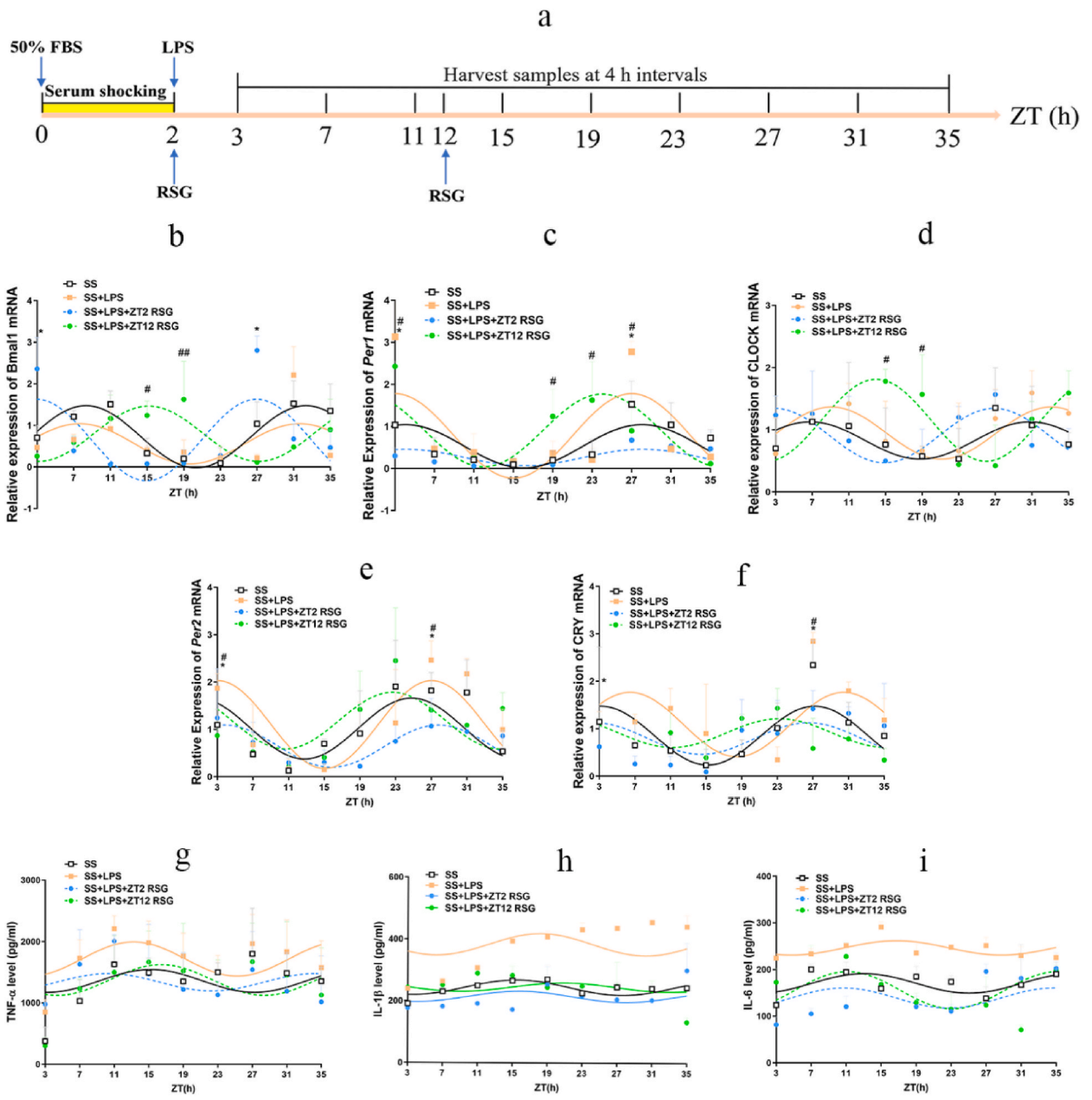

Fig. 1. Chronotherapy of rosiglitazone influence the circadian rhythm of clock genes and inflammatory cytokines in macrophages (Mean ± SD, n = 3).

All macrophages were serum shocking (SS) via incubation with DMEM plus 50 % FBS for 2 hours in order to induce circadian-clock-gene oscillations. Then, LPS (100 ng/ml) was used to induce M1 type macrophages to release inflammatory cytokines. Rosiglitazone (RSG, 20 μmol) was added at ZT2 and ZT12 respectively. Macrophages and culture supernatant were harvested at an interval of every 4 hours within 35 hours. The oscillation of clock gene expression and circadian rhythm of inflammatory cytokines release in each group is represented as: (a) Macrophage treatment and sample collection schematic; (b) Bmal1 gene; (c) Per1 gene; (d) CLOCK gene; (e) Per2 gene; (f) CRY gene; (g) TNF-α; (h) IL-1β; (i) IL-6. SS + LPS vs SS + LPS + ZT2 RSG group cells, *P < 0.05, **P < 0.01; SS + LPS vs SS + LPS + ZT12 RSG group cells, $^{\#}$P < 0.05, $^{\#\#}$P < 0.01.

2.14. Statistical analyze

Relative gene expression and relative protein expression levels are reported as means ± standard deviations. Intergroup means at each time point were compared using one-way analysis of variance. Comparisons between only two groups were analysed via Student-Newman-Keuls q tests. Circadian rhythms were detected by JTK_CYCLE, which is a new algorithm designed to efficiently identify and characterise cycling variables in large datasets. Where p values less than 0.05 indicate the existence of a circadian rhythm. The

Table 1
The parameters of circadian rhythm of clock gene and inflammatory cytokines release in macrophage.

Parameters	SS	SS + LPS	SS + LPS + ZT2 RSG	SS + LPS + ZT12 RSG
Amplitude				
Bmal1	0.75 ± 0.11	0.48 ± 0.18	0.98 ± 0.21*	0.67 ± 0.15
CLOCK	0.30 ± 0.16	0.42 ± 0.14	0.44 ± 0.12	0.66 ± 0.11$^{\#}$
Per1	0.51 ± 0.12	1.01 ± 0.25	0.20 ± 0.07*	0.87 ± 0.17$^{\#}$
Per2	0.64 ± 0.19	0.93 ± 0.19	0.44 ± 0.13*	0.60 ± 0.21$^{\#}$
CRY	0.62 ± 0.18	0.68 ± 0.20	0.33 ± 0.18	0.30 ± 0.13
TNF-α	264.1 ± 88.28**	152.5 ± 112.7	214.3 ± 77.69*	83.07 ± 105.7*$^{\#\#}$
IL-1β	24.03 ± 5.16*	35.12 ± 23.09	17.41 ± 14.72*	14.18 ± 14.68*
IL-6	20.89 ± 9.98	15.41 ± 5.78	21.47 ± 12.53	39.70 ± 14.44*$^{\#}$
Baseline				
Bmal1	0.73 ± 0.08	0.56 ± 0.13	0.65 ± 0.15	0.80 ± 0.10*$^{\#}$
CLOCK	0.83 ± 0.11	0.95 ± 0.10	0.91 ± 0.08	1.15 ± 0.09*$^{\#}$
Per1	0.53 ± 0.09	0.78 ± 0.18	0.26 ± 0.05	0.90 ± 0.12*$^{\#}$
Per2	1.02 ± 0.14	1.10 ± 0.14	0.65 ± 0.10	1.19 ± 0.15
CRY	0.85 ± 0.12	1.09 ± 0.14	0.79 ± 0.13	0.91 ± 0.10
TNF-α	685.2 ± 65.75**	1288 ± 83.84	495.4 ± 55.69*	781.4 ± 76.59*$^{\#}$
IL-1β	244.1 ± 3.77*	383.3 ± 16.36	214.4 ± 10.69*	245.0 ± 10.5*
IL-6	170.1 ± 7.43*	246.1 ± 4.15	138.8 ± 9.18*	155.6 ± 10.63*
Acrophase				
Bmal1	8.30	7.70	2.95	15.17
CLOCK	6.78	9.11	2.88	13.99
Per1	4.06	3.01	4.10	24.00
Per2	0.79	3.05	3.81	22.64
CRY	3.19	6.46	2.46	23.22
TNF-α	13	12.3	9.1	16.06
IL-1β	15.6	18.3	15.9	20.92
IL-6	13	16.76	10.7	11.2

Relative gene expression values and inflammatory factor values were fit with least square method by using GraphPad Prism. The baselineis a measurement of the average expression level around which the curve oscillates over time, usually called mesor. Amplitude is the change in expression at high and low points relative to the corresponding baseline. Circadian rhythm parameters were expressed as the means value ± standard error, and comparisons between the two groups were performed by using the extra sum of squares test. *P < 0.05, **P < 0.01 vs SS + LPS group; $^{\#}$P < 0.05,$^{\#\#}$P < 0.01, vs SS + LPS + ZT2 RSG group.

procedure of JTK_CYCLE was operated in R, a statistical language. Relative gene expression and relative protein expression values were fit with the following equation via GraphPad Prism:

$$Y = \text{Amplitude} \times \cos [0.2618 \times (X - \text{Phase})] + \text{Baseline}$$

where “Baseline” is the measurement of the average expression level around which the curve oscillates over time (usually called mesor); and “Amplitude” denotes the change in expression at high and low points relative to the corresponding baseline. Circadian rhythm parameters are expressed as means ± standard error of the means, and comparisons between two groups were performed by using the extra sum of squares test (Luan et al., 2022). The extra sum of squares test is the most commonly used method to discriminate parameters between different non-linear fitting models (https://www.graphpad.com/guides/prism/7/curve-fitting/index.htm).

3. Results

3.1. The chronotherapy involving RSG induces phase shifts in both clock genes and TNF-α

In this experiment, we employed LPS to induce the expression of inflammatory factors in RAW264.7 macrophages after cell synchronization via 50 % FBS shocking for 2 hours. Our objective was to investigate the expression patterns of clock genes and the release patterns of inflammatory factors following time-dependent administration of RSG (at ZT2 and ZT12) at 4-hour intervals. The schematic diagram of the experimental setup is shown in Fig. 1 a. As depicted in Fig. 1, the administration of RSG at ZT2 resulted in a significant increase in Bmal1 gene expression at ZT3 and ZT27. However, the expression of Per1, Per2, and CRY genes appeared to be suppressed at either ZT3 or ZT27, consistent with the transcription-translation negative feedback loop of the clock system. On the other hand, RSG administration at ZT12 led to a marked increase in Bmal1 and CLOCK gene expression at ZT15 and ZT19. At these time points, the expression levels of Per1, Per2, and CRY genes were relatively lower compared to the SS + LPS group cells (Fig. 1 b-f). These findings resulted in a phase forward shift of the core clock genes Bmal1 and CLOCK after ZT2 administration of RSG, while ZT12 administration induced a phase backward shift compared to the SS + LPS group cells. Although we observed significant differences in amplitude and baseline, we did not focus on these factors in this study (Table 1).

Previous research has demonstrated that the circadian rhythm of inflammatory factor secretion in macrophages is regulated by the clock system. Consequently, we examined the circadian rhythms of TNF-α, IL-1β, and IL-6 in macrophages following time-dependent administration of RSG. As anticipated, the phases of TNF-α and IL-1β were shifted forward after ZT2 administration of RSG but

Table 2
The circadian release rhythm of flammatory cytokines in macrophage.

inflammatory factors	SS	SS + LPS	SS + LPS + ZT2 RSG	SS + LPS + ZT12 RSG
TNF-α	<0.05	<0.05	<0.05	<0.05
IL-1β	NA	NA	NA	NA
IL-6	<0.05	NA	NA	<0.05

The existence of circadian rhythm was detected by JTK_CYCLE, which the P value was less than 0.05 indicating the existence of circadian rhythm (also called zero-amplitude test).

backward after ZT12 administration compared to the SS + LPS group cells (Fig. 1 g-h; Table 1). The expression rhythm of IL-6 did not exhibit a similar pattern (Fig. 1 i). Nevertheless, the zero-amplitude test revealed that there was no rhythmicity in the release of IL-1β by macrophages (Table 2). Furthermore, significant differences in amplitude and baseline were observed between ZT2 and ZT12 administration of RSG, and since RSG demonstrated direct anti-inflammatory effects in this experiment, we did not focus on these factors.

In summary, our results indicate that ZT2 administration of RSG advances the phase of core clock genes, whereas ZT12 administration delays the phase of these genes, with TNF-α exhibiting synchronous rhythmic changes.

3.2. TNF-α phase shift regulates VSMC phenotypic switch

To emulate the variable phase patterns of TNF-α release by macrophages, we established a co-culture system of VSMCs and macrophages (Fig. 2 a). In this system, cell communication occurs only through secreted factors. We stimulated macrophages with RSG at ZT2 or ZT12 and used a TNF-α-neutralizing antibody (nTNF-α) to observe if TNF-α plays a decisive role. The results showed that the cell number of VSMCs were significant higher after macrophages treated with RSG at ZT2 rather than ZT12. The nTNF-α significantly abolished this difference (Fig. 2 b-c). So, we designed an experimental plan to verify the effect of timed administration of TNF-α on VSMCs' phenotypic transition (Fig. 2 d). VSMCs were exposed to recombinant TNF-α protein at different time points following serum shocking, as previously described. The results, depicted in Fig. 2, reveal noteworthy insights. When VSMCs were incubated with gradient concentrations of TNF-α at ZT2 within 24hours , there was a substantial increase in the cellular viability. Intriguingly, this effect was utterly nullified when the incubation occurred at ZT12. At other time points of incubation, the proliferative impact of TNF-α was more modest (Fig. 2 e).

Complementary evidence from ki67 assays, cell scratch assays and transwell experiments further solidified these findings. The ki67 experiment showed that adding TNF-α at ZT2 significantly increased the proliferation activity of VSMCs, but there was no significant difference in proliferation between groups when TNF-α was added at ZT12 (Fig. 2 f. i). Cell scratch assays and transwell experiments demonstrated that the addition of TNF-α at ZT2 maintained VSMCs at a heightened level of migration. Conversely, when TNF-α was introduced at ZT12, its ability to stimulate the phenotypic transition of VSMCs was entirely abrogated (Fig. 2 g-i). Collectively, these studies underscore the profound impact of incubating VSMCs with TNF-α at different times on eliciting distinct phenotypic changes. Incubation with TNF-α at ZT2 facilitates the transition of VSMCs, while this effect diminishes when incubation occurs at ZT12. Consequently, the phase shift in TNF-α released by macrophages, achieved through the chronotherapy with RSG, emerges as a key regulator in orchestrating the phenotypic switch of VSMCs.

3.3. TNF-α phase shift regulates clock genes and MAPK signal pathway in VSMCs

In our previous research, we established that the clock system orchestrates the MAPK pathway to control the phenotypic switch in VSMCs [15]. To further investigate whether the time-dependent incubation of VSMCs with TNF-α modulates this phenotypic switch through the clock-MAPK pathway, we assessed the expression patterns of clock genes and core MAPK proteins. When TNF-α was added at ZT2, there was a significant inhibition of Bmal1 expression at ZT3, ZT23, and ZT27 (Fig. 3 a). This inhibition appears to be linked to the substantial increase in Per1 and Per2 expression at ZT3, as well as CRY expression at ZT7, ZT11, and ZT27 (Fig. 3 c-e). Conversely, adding TNF-α at ZT12 significantly inhibited Bmal1 expression at ZT15 and ZT19 (Fig. 3 a). In this case, Per1 expression significantly increased at ZT15 and ZT19, while Per2 gene expression increased at ZT19, and CRY gene expression increased at ZT15 (Fig. 3 c-e). The primary disparity between ZT2 and ZT12 administrations in terms of clock gene rhythm parameters in VSMCs pertains to the baseline changes of Per1 and Per2 (Table 3).

Proliferating Cell Nuclear Antigen (PCNA) is a crucial molecule in cells, essential for maintaining DNA integrity, stability, and normal cell cycles. PCNA is often utilized as a biomarker for VSMC proliferation. We observed a significant increase in PCNA protein expression in VSMCs when TNF-α (200 ng/ml) was added at ZT2. However, this increase was absent when gradient concentrations of TNF-α were added at ZT12. Regarding the MAPK pathway, TNF-α (25 ng/ml) led to a significant increase in ERK phosphorylation, and TNF-α (100 and 200 ng/ml) resulted in significant MEK phosphorylation when added at ZT2 in VSMCs. Conversely, when TNF-α was added at the ZT12 time point, the expression of these proteins remained unchanged (Fig. 3 f-i).

These findings strongly suggest that the phase shift in TNF-α, induced by RSG chronotherapy in macrophages, regulates the phenotypic switch in VSMCs through the clock-MAPK signaling pathway.

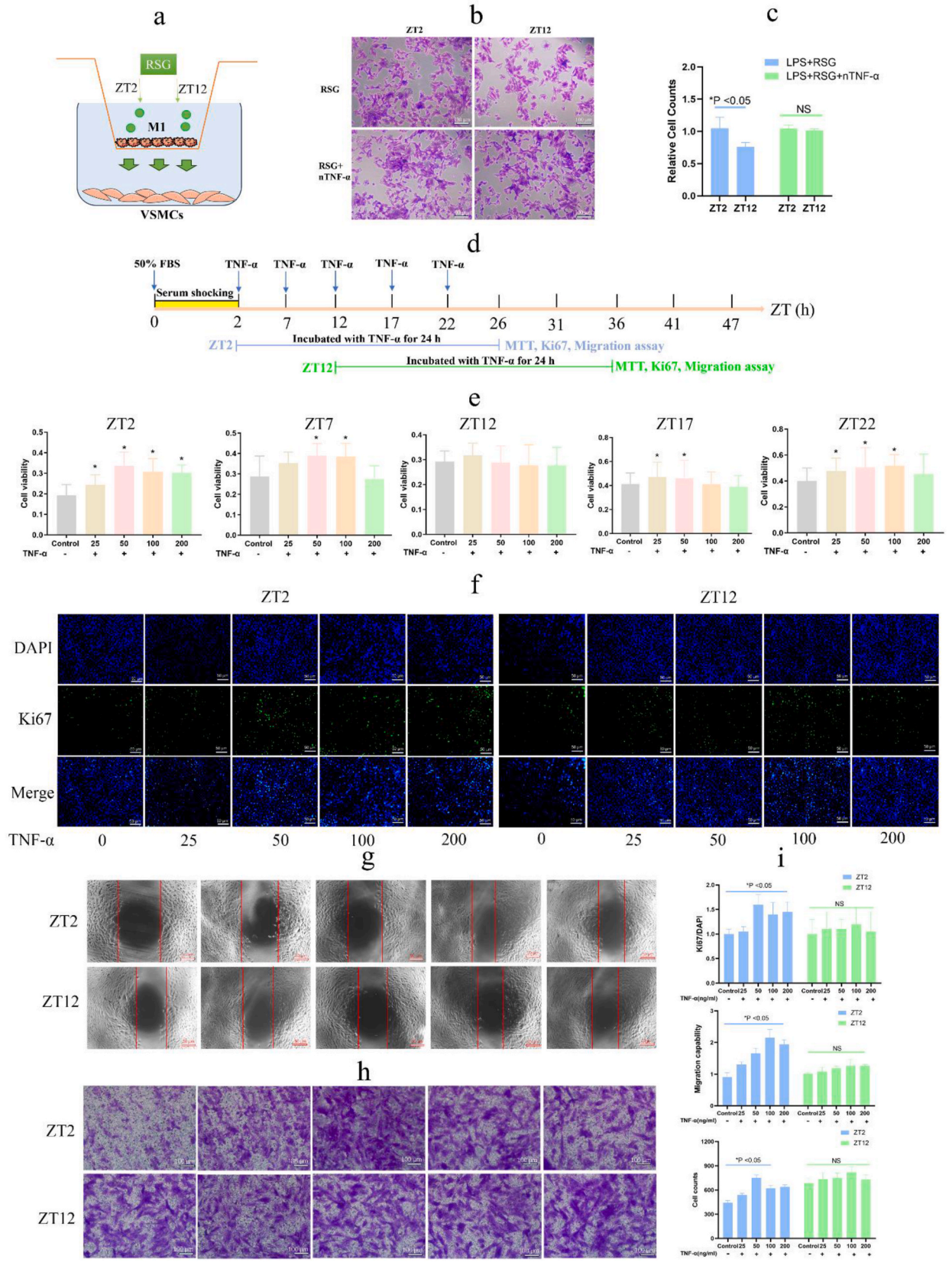

(caption on next page)

Fig. 2. The TNF-α added at different times regulate the phenotype switch of vascular smooth muscle cells (Mean ± SD, n = 3).
The co-culture system of vascular smooth muscle cells (VSMCs) and macrophages, along with the use of TNF-α-neutralizing antibodies (nTNF-α, 1 μg/ml), was employed to confirm the critical role of TNF-α. After this, VSMCs were shocking via incubated with DMEM plus 50 % FBS. The initial time of serum shocking (SS) is recorded as ZT0. After 2 hours of incubation, the time is recorded as ZT2. TNF-α (100 ng/ml) were added at ZT2, ZT7, ZT12, ZT17 and ZT22, respectively. All cells must be co cultured with TNF-α for 24 hours before harvest cells. The cell viability was shown as following: (a) The co-culture system of VSMCs and macrophages; (b) After adding RSG at different time points in upper chamber, the VSMCs in the co-culture system were stained with crystal violet in the lower chamber (× 100); (c) The quantitative analysis of 'b'; (d) VSMCs treatment and sample collection schematic; (e) MTT assay after different time incubated with TNF-α; (f) Ki67 assay after different time incubated with TNF-α (× 50); (g) Wounding healing assay after adding TNF-α at ZT2 and ZT12, respectively (× 50); (h) Transwell assay after adding TNF-α at ZT2 and ZT12, respectively (× 100). (i) The quantitative analysis of 'e', 'g' and 'h'; *P < 0.05, **P < 0.01 vs Control group cells.

3.4. RSG chronotherapy shifts the phase of PPARγ and Bmal1 proteins

Here, we can tentatively summarize that treating macrophages with RSG at different time points leads to a phase shift in TNF-α secretion of macrophages, and this phase shift can regulate the phenotypic transition of VSMCs. However, the underlying mechanism remains unclear. RSG is a classic PPARγ agonist and has a regulatory effect on the biological clock of macrophages, indicating a potential interaction between PPAR gamma and clock genes (Bmal1). To investigate this, we examined the circadian expression patterns of PPARγ and Bmal1 proteins following RSG chronotherapy in macrophages. Upon administering RSG at ZT2, we observed a significant increase in PPARγ protein expression at ZT7 and ZT11, accompanied by a significant increase in Bmal1 protein expression at ZT7 and ZT15 (Fig. 4 a). Conversely, after ZT12 administration of RSG, both PPARγ and Bmal1 proteins exhibited a slight up-regulation at ZT27 and ZT31, although the differences were not statistically significant (Fig. 4 b-c). It is worth noting that despite the lack of statistical significance, this subtle up-regulation remains meaningful as it results in a backward delay in the phase of PPARγ and Bmal1 proteins. In contrast, ZT2 administration of RSG advanced the phase of both PPARγ and Bmal1 proteins. Importantly, no significant differences were observed in amplitude and baseline between the ZT2 and ZT12 administration groups of RSG (Table 4).

These results strongly suggest that PPARγ agonists induce the up-regulation of PPARγ and shift its phase forward or backward depending on the time of administration. Additionally, Bmal1 exhibits synchronized changes with PPARγ, implying a close relationship between these two proteins.

3.5. PPARγ does not directly regulate Bmal1 expression in macrophages

The specific relationship between Bmal1 and PPAR gamma is still unclear. To elucidate this, we employed siRNA and plasmid transfection techniques to both knock down and overexpress PPARγ. As depicted in Fig. 5 a, siRNA-1 exhibited the most effective silencing efficiency. On the other hand, plasmid transfection resulted in PPARγ expression levels exceeding 1500 times that of the NC group cells within 48 hours (Fig. 5 b). However, after either silencing or overexpressing PPARγ, there were no significant differences observed in the expression levels of Bmal1, Per1, and CRY genes (Fig. 5 c, e, g). Specifically, PPARγ silencing only led to a decrease in CLOCK gene expression, while PPARγ overexpression only increased the expression of the Per2 gene (Fig. 5 d, f). In this experiment, we parallelly tested the levels of PPARγ gene after silencing and overexpression, reaffirming the experimental reliability (Fig. 5 h). These findings strongly suggest that PPARγ does not exert direct regulatory control over the expression of Bmal1 in macrophages.

3.6. PPARγ May induce Bmal1 expression via PAL and TG accumulation in macrophages

Considering that PPARγ is a well-known regulator of lipid metabolism, known for its capacity to promote the absorption, synthesis, and storage of lipids, it is plausible that increased PPARγ expression could result in lipid accumulation within cells, subsequently impacting the expression of clock genes. To explore this hypothesis, we introduced 10 % mouse serum (10 % MS) into the cell culture medium. This addition allowed for more lipids to enter the cells when PPARγ was active. It's worth noting that the presence of 10 % MS significantly influenced the expression of clock genes, with Per1, Per2, and CRY showing significant increases, while Bmal1 exhibited significant suppression (Fig. 6 a). Furthermore, the introduction of a control (NC) plasmid did not produce any additional impact on clock genes. However, as anticipated, overexpression of PPARγ resulted in an approximate threefold increase in the expression of Bmal1 and CLOCK genes compared to the NC group cells. Additionally, this led to a significant decrease in the expression of Per1, Per2, and CRY (Fig. 6 a). This demonstrates that PPARγ overexpression had a substantial influence on the clock gene expression patterns. We also evaluated the expression levels of PPARγ and Bmal1 proteins. Similar to gene expression, there is a significant increase in their levels after PPARγ overexpression in macrophages (Fig. 6 b).

To understand which specific lipid substances synthesized in macrophages lead to changes in clock gene expression after PPARγ overexpression, we tested five representative lipid substances in macrophages, namely LA, PAL, DAG, TG, and cholesterol. Total cholesterol and free cholesterol concentrations were too low to be detected (not shown). Moreover, there was no significant difference observed in the concentration of LA and DAG between the NC and PPAR overexpression groups (Fig. 6 c, e). However, we did observe a significant increase in intracellular PAL and TG concentrations after PPARγ overexpression, respectively (Fig. 6 d, f).

These findings collectively suggest that PPARγ may induce the expression of Bmal1 through the accumulation of PAL and TG in macrophages.

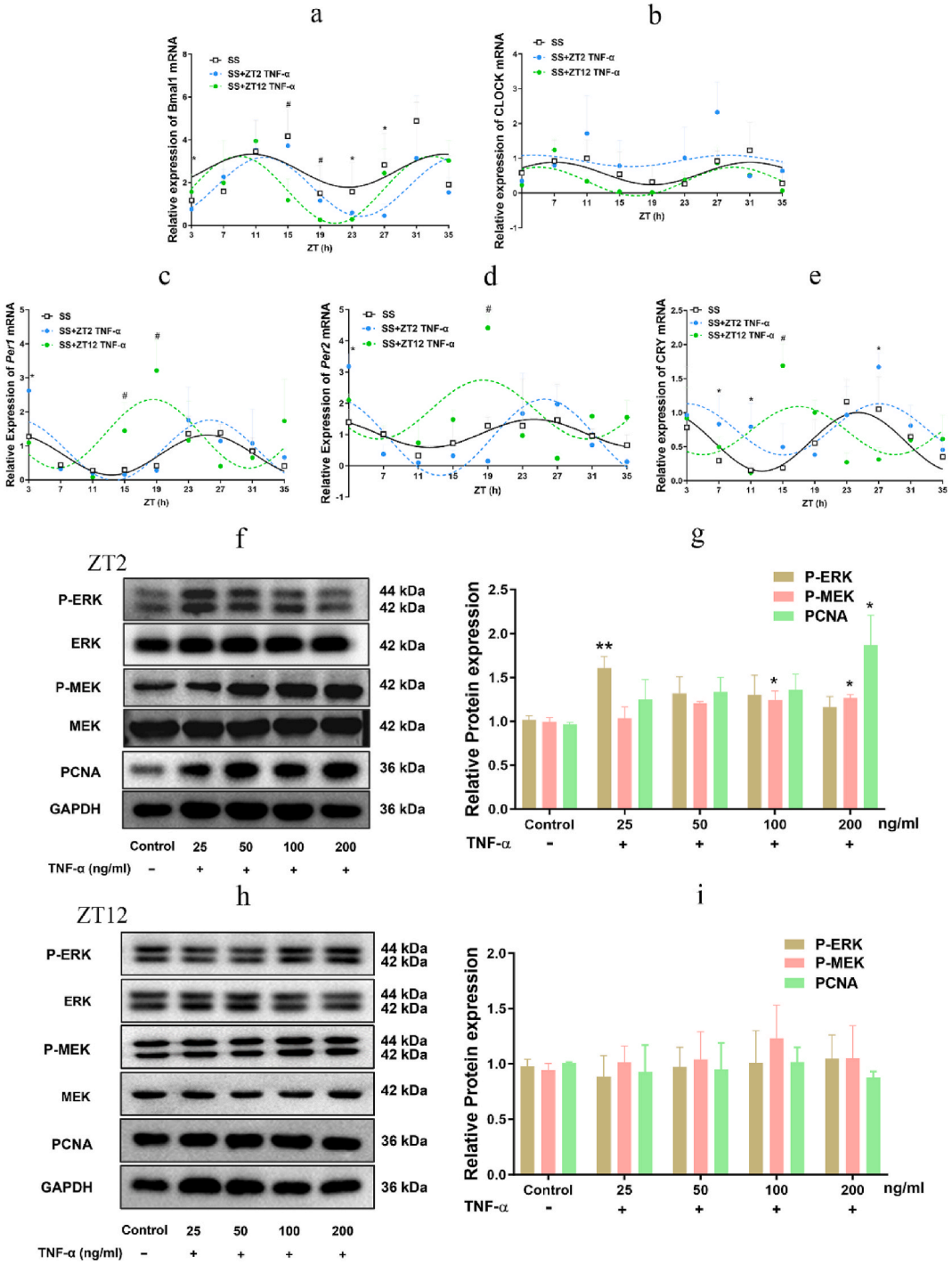

Fig. 3. The TNF-α added at different times regulate circadian rhythm of clock genes and MAPK pathway (Mean ± SD, n = 3).
All vascular smooth muscle cells (VSMCs) were serum shocking (SS) via incubated with DMEM plus 50 % FBS in order to induce circadian-clock-gene oscillations. TNF-α (100 ng/ml) were added at ZT2 and ZT12 after SS, respectively. Vascular smooth muscle cells (VSMCs) were harvested at an interval of every 4 hours within 35 hours. The circadian oscillation of clock gene expression in each group is represented as: (a) Bmal1 gene; (b) CLOCK gene; (c) Per1 gene; (d) Per2 gene; (e) CRY gene; (f) The relative expression of ERK and MEK phosphorylation level, PCNA after adding TNF-α at ZT2. (g) The quantitative analysis of 'f'. (h) The relative expression of ERK and MEK phosphorylation level, PCNA after adding TNF-α at ZT12. (i) The quantitative analysis of 'h'. SS vs SS + ZT2 TNF-α group cells, *P < 0.05, **P < 0.01; SS vs SS + ZT12 TNF-α group cells, $^{\#}$P < 0.05, $^{\#\#}$P < 0.01.

Table 3
The parameters of circadian rhythm of clock genes in vascular smooth muscle cells.

Genes	SS	SS + ZT2 TNF-α	SS + ZT12 TNF-α
Amplitude			
Bmal1	0.77 ± 0.41	1.38 ± 0.43	1.57 ± 0.33*
CLOCK	0.32 ± 0.12	0.17 ± 0.25	0.41 ± 0.10
Per1	0.59 ± 0.08	0.88 ± 0.18	1.01 ± 0.25*
Per2	0.45 ± 0.19	1.22 ± 0.20**	0.94 ± 0.31*
CRY	0.43 ± 0.10	0.38 ± 0.09	0.35 ± 0.13
Baseline			
Bmal1	2.55 ± 0.30	1.80 ± 0.30**	1.67 ± 0.22**
CLOCK	0.56 ± 0.08	0.92 ± 0.18	0.33 ± 0.07
Per1	0.73 ± 0.06	0.88 ± 0.14	1.36 ± 0.18**$^{\#\#}$
Per2	1.04 ± 0.14	0.92 ± 0.15	1.80 ± 0.22**$^{\#\#}$
CRY	0.57 ± 0.07	0.75 ± 0.07	0.74 ± 0.09
Acrophase			
Bmal1	10.5	12	8.88
CLOCK	7.06	4.36	5.08
Per1	1.38	1.70	18.56
Per2	0.31	1.52	18.46
CRY	0.42	3.08	17

Relative gene expression values were fit with least square method by using GraphPad Prism. The baseline is a measurement of the average expression level around which the curve oscillates over time, usually called mesor. Amplitude is the change in expression at high and low points relative to the corresponding baseline. Circadian rhythm parameters were expressed as the means value ± standard error, and comparisons between the two groups were performed by using the extra sum of squares test. *P < 0.05, **P < 0.01 vs SS group; $^{\#}$P < 0.05,$^{\#\#}$P < 0.01, vs SS + ZT2 TNF-α group.

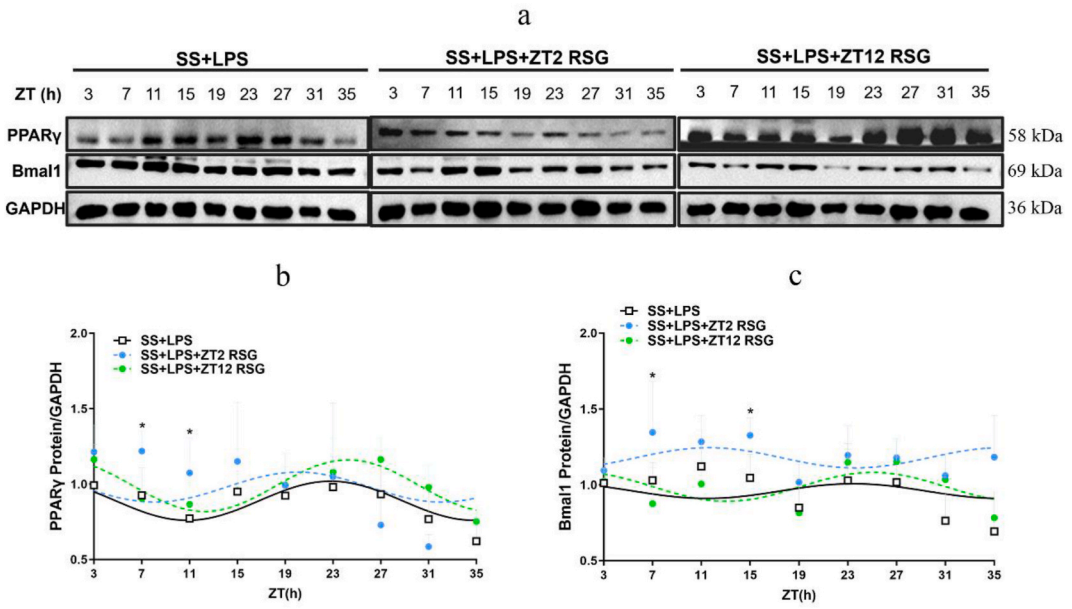

Fig. 4. Chronotherapy of rosiglitazone influence the circadian rhythm of PPARγ and Bmal1 in macrophages (Mean ± SD, n = 3).
All macrophages were serum shocking (SS) via incubated with DMEM plus 50 % FBS in order to induce circadian-clock-gene oscillations. Then LPS (100 ng/ml) were used to induce M1 type macrophages. Rosiglitazone (RSG, 20 μmol) were added at ZT2 and ZT12 respectively. Macrophages were harvested at an interval of every 4 hours within 35 hours. (a) The circadian oscillation of PPARγ and Bmal1 proteins in each group; (b) The quantitative analysis of PPARγ protein in each group; (c) The quantitative analysis of Bmal1 protein in each group. SS + LPS vs SS + LPS + ZT2 RSG group cells, *P < 0.05, **P < 0.01; SS + LPS vs SS + LPS + ZT12 RSG group cells, $^{\#}$P < 0.05, $^{\#\#}$P < 0.01.

3.7. TG plays a vital role in regulating the clock system in macrophages

To underscore the impact of PAL and TG on the expression of clock genes, we initiated an investigation. First, we examined the intracellular concentrations of PAL and TG after incubating macrophages with gradient concentrations (1, 10, 100 ng/ml) of PAL and TG. Following the addition of PAL, we observed a significant decrease in the intracellular concentration of PAL within 24 h and 48 h (Fig. 7 a). Conversely, TG successfully accumulated within macrophages after the addition of gradient concentrations of TG within the

Table 4
The parameters of circadian rhythm of PPARγ and Bmal1 protein in macrophage.

Genes	SS + LPS	SS + LPS + T2 RSG	SS + LPS + T12 RSG
Amplitude			
PPARγ	0.13 ± 0.04	0.12 ± 0.09	0.17 ± 0.04
Bmal1	0.05 ± 0.05	0.07 ± 0.05	0.10 ± 0.04
Baseline			
PPARγ	0.89 ± 0.03	0.97 ± 0.06	0.99 ± 0.03
Bmal1	0.96 ± 0.04	1.18 ± 0.03*	0.99 ± 0.03
Acrophase			
PPARγ	22.82	19.91	24.26
Bmal1	23.44	11.61	25.07

Relative protein expression values were fit with least square method by using GraphPad Prism. The baselineis a measurement of the average expression level around which the curve oscillates over time, usually called mesor. Amplitude is the change in expression at high and low points relative to the corresponding baseline. Circadian rhythm parameters were expressed as the means value ± standard error, and comparisons between the two groups were performed by using the extra sum of squares test. *P < 0.05, vs SS + LPS group.

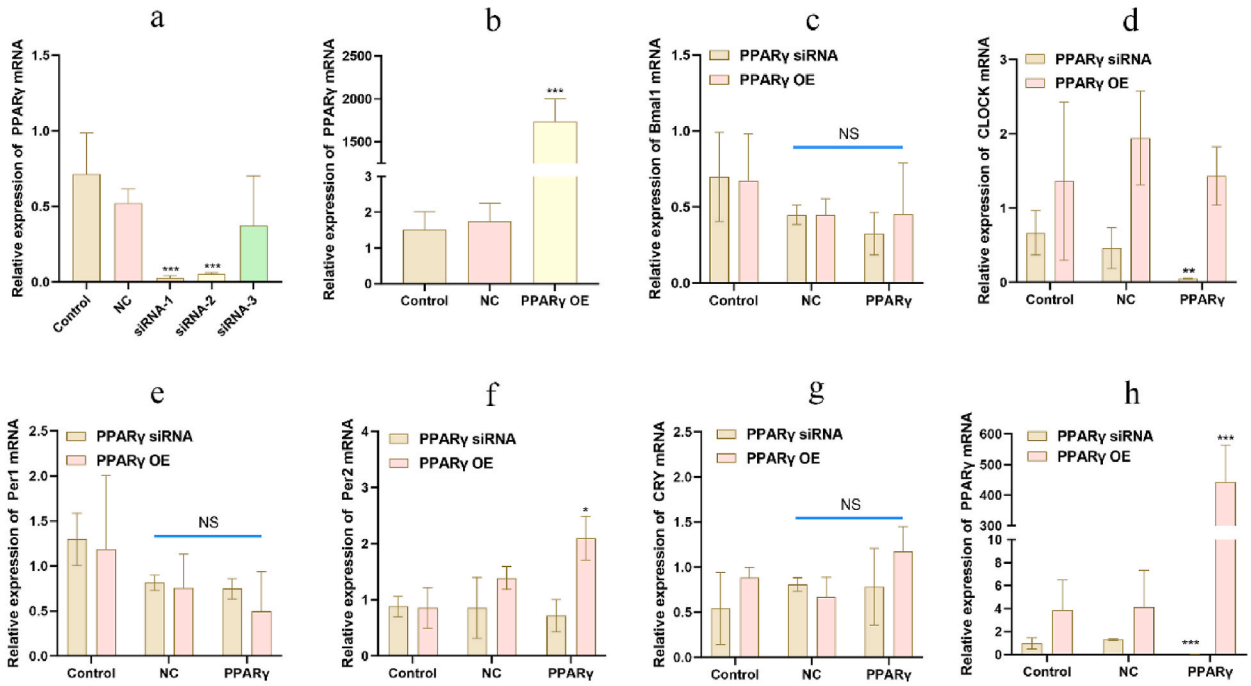

Fig. 5. The relative expression of clock genes after silence or overexpression of PPARγ in macrophages (Mean ± SD, n = 3).
PPARγ were silenced via transfection of siRNA (50 nmol) and overexpressed via transfection of plasmid contain PPARγ gene sequence (100 nmol). After 48 h, macrophages were collected. (a) The silence efficiency of PPARγ among three siRNA sequence; (b) The overexpression level of PPARγ after transfection; (c) The relative expression of Bmal1 gene; (d) The relative expression of CLOCK gene; (e) The relative expression of Per1 gene; (f) The relative expression of Per2 gene; (g) The relative expression of CRY gene; (h) The relative expression of PPARγ gene; *P < 0.05, **P < 0.01, ***P < 0.001 vs NC group cells.

same time frame (Fig. 7 b). Moreover, both PAL and TG were found to induce the release of TNF-α in macrophages (Fig. 7 c-d). However, the addition of PAL to macrophages resulted in a significant decrease in the expression of clock genes, including Bmal1, Per1, Per2, and CRY, indicating that the PAL disrupts the overall circadian system (Fig. 7 e). In contrast, the addition of TG to macrophages led to a significant increase in the expression of Bmal1 and CLOCK genes, while the expression of Per1, Per2, and CRY was suppressed, indicating that the circadian system can function normally (Fig. 7 f). At the protein level, in line with the trends observed in gene expression, PAL decreased the expression of Bmal1, while TG increased it (Fig. 7 g). These findings collectively suggest that following PPARγ activation, the regulation of the circadian clock system may be achieved through the promotion of TG accumulation within the cells.

4. Discussion

Controlling the phenotypic switch in VSMCs is an effective strategy for treating CVDs. Additionally, given the intercellular

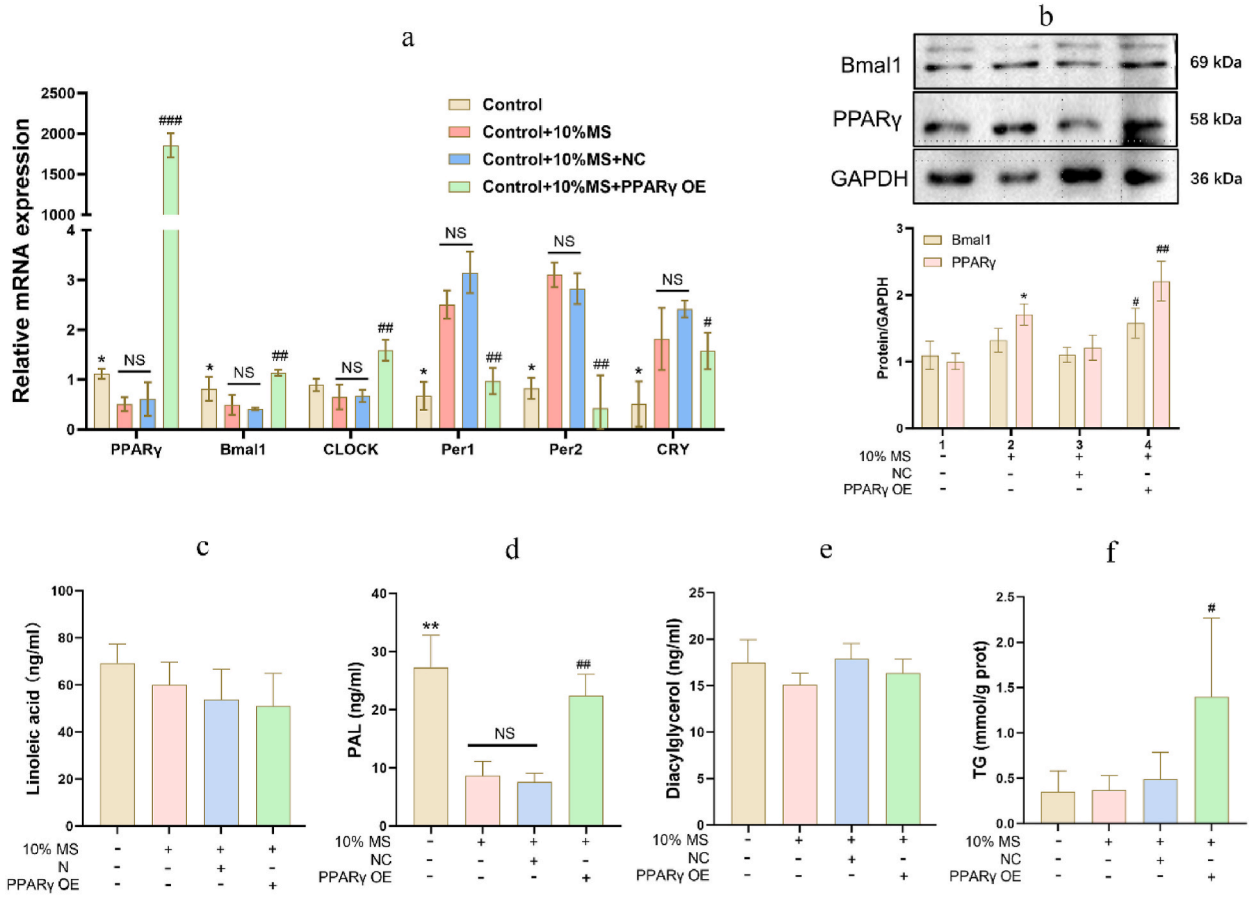

Fig. 6. The relative expression of clock genes and intracellular lipid after overexpression of PPARγ in macrophages (Mean ± SD, n = 3). PPARγ were overexpressed via transfection of plasmid contain PPARγ gene sequence (100 nmol). After 48 h, macrophages were collected. (a) The relative expression of clock genes after overexpression of PPARγ; (b) The relative expression of PPARγ and Bmal1 protein after overexpression of PPARγ; (c) Intracellular level of linoleic acid; (d) Intracellular level of palmitic acid (PAL); (e) Intracellular level of diacylglycerol; (f) Intracellular level of triglyceride (TG). Control vs Control+10%MS, *P < 0.05, **P < 0.01; Control+10%MS + NC vs Control+10%MS + PPARγ OE, $^{\#}$P < 0.05, $^{\#\#}$P < 0.01, $^{\#\#\#}$P < 0.01.

communication between macrophages and VSMCs, identifying effective methods to modulate macrophage secretory functions holds the potential to control VSMCs' phenotypic transitions. In this study, we employed chronotherapy with the PPARγ agonist RSG to treat LPS-induced macrophages. Our findings can be summarized as follows: (i) RSG administration at ZT2 significantly advanced the phase of TNF-α secretion, while ZT12 administration caused a backward shift in TNF-α phase. These distinct temporal impacts influence VSMC phenotypic transitions via the clock-MAPK pathway. (ii) Unlike direct transcriptional promotion of Bmal1 by PPARγ, PPARγ activation accelerates the accumulation of TG in macrophages. This, in turn, significantly induces the expression of Bmal1 and TNF-α.

Various methods of chronotherapy exist, encompassing adjustments in medication timing and dosage, light therapy, targeting clock genes, and sleep-wake schedule modifications [16–18] [16–18] [16–18]. In the realm of pharmaceutical treatment, chrono-modulated drug delivery stands out as the prevailing form of chronotherapy. For instance, administering antihypertensive drugs before bedtime has demonstrated its efficacy in managing hypertension and circadian blood pressure rhythms, ultimately reducing CVD risks [19]. Additionally, our research has unveiled how valsartan chronotherapy can reshape the circadian rhythm of the renin-angiotensin system (RAS), influencing blood pressure patterns [20]. Further investigation has revealed that VSMCs respond differently to angiotensin II based on the oscillations of clock genes [20]. Inspired by these insights, we explored whether VSMCs exhibit varying sensitivities to the circadian rhythm of inflammatory factors released by macrophages. As anticipated, chronotherapy-induced phase changes in TNF-α release yielded fundamental differences in the phenotypic switching of VSMCs. This implies that the circadian clock system, particularly the Bmal1 gene, creates a temporal window of opportunity for the effectiveness of drugs and internal endocrine regulators. In essence, the expression levels of clock genes can significantly influence the actions of drugs and cytokines. For example, Bmal1 gene knockout exacerbates *propionibacterium acnes*-induced skin inflammation, and Bmal1 downregulation worsens *porphyromonas gingivalis*-induced atherosclerosis [21]. Our research further demonstrates that VSMCs exhibit heightened sensitivity to TNF-α when Bmal1 expression is relatively higher (Fig. 3 a). By comprehending the rhythmic oscillations of circadian clock genes,

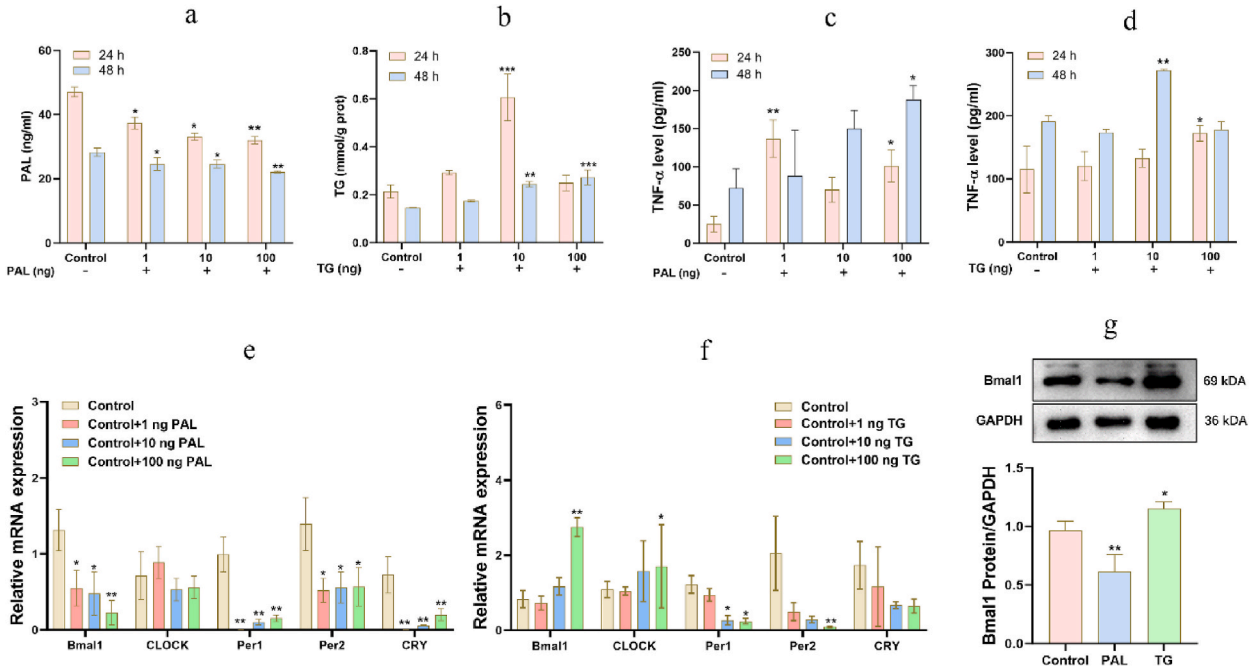

Fig. 7. PAL and TG influence the relative expression of clock genes and TNF-α release in macrophages (Mean ± SD, n = 3).
Macrophages were incubated with gradient concentration of palmitic acid (PAL) (1, 10, 100 ng/ml) and triglyceride (TG) (1, 10, 100 ng/ml). After 24 h and 48 h, the macrophages and cell culture supernatant were collected. (a) Intracellular level of PAL; (b) Intracellular level of TG; (c) TNF-α level in cell supernatant after adding gradient concentration of PAL; (d) TNF-α level in cell supernatant after adding gradient concentration of TG; (e) The relative expression of clock genes after adding gradient concentration of PAL; (f) The relative expression of clock genes after adding gradient concentration of TG; (g) The relative expression of Bmal1 after adding PAL (100 ng/ml) and TG (100 ng/ml). *P < 0.05, **P < 0.01 vs Control group cells.

determining the optimal timing for medication intake becomes a powerful tool to enhance therapeutic effectiveness and reduce adverse effects.

Clock genes play a pivotal role in the realm of chronotherapy. This involves two primary aspects: firstly, as previously mentioned, targeting circadian clock genes can either enhance or diminish the efficacy of drugs. Secondly, the development and progression of certain diseases are intricately linked to disruptions in circadian clock genes. Consequently, targeting these clock genes can directly impact the treatment of these diseases [22,23]. For instance, circadian rhythm disorders have been shown to elevate cytokine release from macrophages and induce dysfunction across multiple organs in mice [24,25] [[,][25]]. The knockout of Bmal1 in VSMCs exacerbates carotid atherosclerotic lesions [26], while the CLOCK gene accelerates atherosclerosis by promoting endothelial autophagy [27]. Furthermore, it has been reported that clock genes in macrophages control the release of cytokines or chemokines [28–30]. Therefore, targeting clock genes to modulate the circadian rhythm in macrophages holds potential as a therapeutic approach for various diseases. However, the majority of research has primarily focused on the impact of changes in the levels of Bmal1 and clock-controlled cytokines or chemokines in disease development [26,29,31] [[,][29]] [[,][26]]. Our research has uncovered a significant shift in the phases of Bmal1 and TNF-α at ZT2 and ZT12 following the administration of RSG. These changes in the phase of TNF-α rhythm exert control over the phenotypic switching of VSMCs. Our findings highlight that targeting Bmal1 in macrophages to regulate the rhythm of TNF-α release represents an effective approach to treating CVDs driven by VSMCs. This discovery complements the existing body of research on the role of clock gene phases in disease development and treatment processes.

Addressing the clock system poses significant challenges. While it is well-established that light and feeding patterns can influence circadian rhythms through neurological and hormonal mechanisms [32], these methods for modulating the body's circadian rhythms in disease treatment remain largely impractical [33–35]. Recently, attention has turned to the development of pharmacological compounds designed to target Rev-erb and ROR nuclear receptors within the circadian mechanism, offering potential clinical applications [36–38] [36–38] [36–38]. The administration of Rev-erbα agonists to mice has shown promise in treating metabolic disorders and improving inflammatory processing [39–41] [39–41] [39–41]. Additionally, various micro-RNAs have been identified that target Bmal1 to regulate circadian rhythms [42–44] [42–44] [42–44]. However, there is limited research on drugs directly stimulating the Bmal1 gene. Although it has been reported that PPARγ can promote Bmal1 transcription through PPRE elements [14], our study did not reveal a direct interaction between the two (Fig. 5). Bmal1, on one hand, regulates TG synthesis by transactivating the Dgat2 gene, encoding the triacylglycerol synthesis enzyme DGAT2 [45]. On the other hand, raw materials for TG synthesis, such as free fatty acids, exert regulatory effects on clock genes [46,47] [[,][47]]. Our research has shown that the intracellular TG production, facilitated by PPARγ activation, significantly influences the expression rhythm of the Bmal1 gene (Fig. 7). This pathway may underlie the

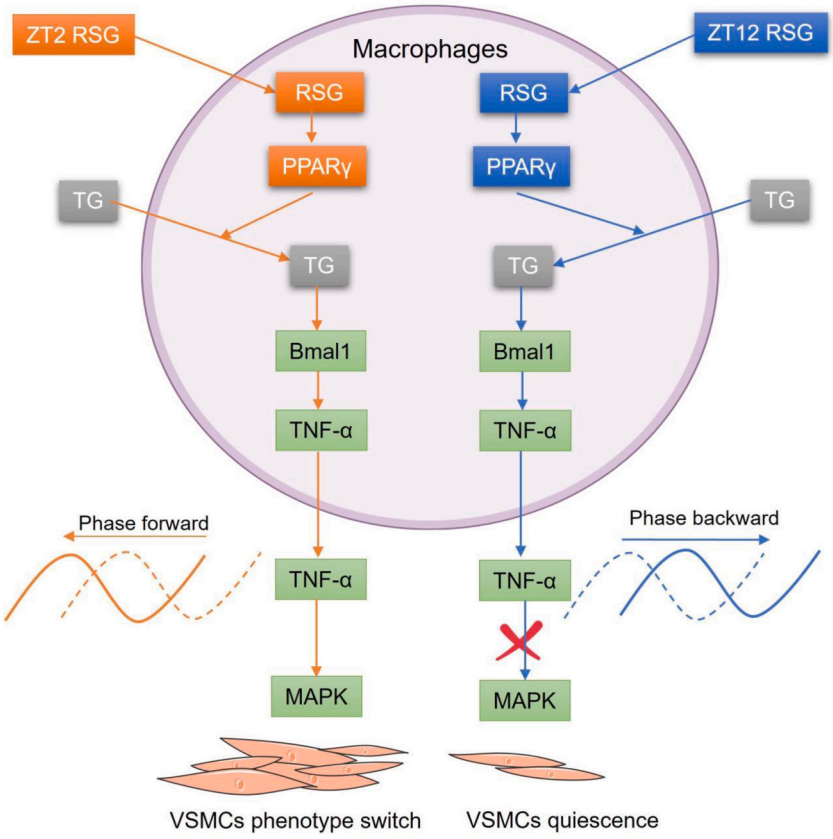

Fig. 8. The mechanism of chronotherapy of rosiglitazone towards to macrophages regulates VSMCs phenotype switch.
Macrophages incubated with rosiglitazone (RSG) at different time (ZT2 and ZT12, respectively) induce the activation of peroxisome proliferator-activated receptor gamma (PPARγ), which promote the accumulation of triglyceride (TG). Then the TG facilitate the expression of basic helix-loop-helix ARNT like 1 (Bmal1), which shift phase forward of TNF-α release rhythm by ZT2 administration of RSG and shift phase backward of TNF-α release rhythm by ZT12 administration of RSG. Finally, the difference between phase of TNF-α release rhythm show an disparate impact on VSMCs phenotype switch via activating or inactive MAPK signal pathway.
Note. Arrow: promote; Dashed line: TNF-α rhythm before administration; Dashed line: TNF-α rhythm before administration; Solid-line curve: TNF-α rhythm after administration.

pharmacological impact of RSG in regulating clock genes within macrophages.

While there are documented reports highlighting PAL, a typical unsaturated long-chain fatty acid found in plants, as a regulator of the circadian clock [48], our research has revealed notable distinctions in how PAL and TG regulate the circadian clock within macrophages. When TG is introduced to macrophages, the circadian clock's TTFL pathway remains functional. Conversely, the addition of PAL results in the suppression of all related circadian clock genes in macrophages, indicating a disruption of the circadian clock system, suggesting the lipotoxic effects of PAL. Macrophages that phagocytose lipids may enter a foamy state, potentially contributing to disease progression [49]. However, in our study, we propose that the appropriate accumulation of TG within macrophages is a normal occurrence that can regulate the rhythmicity of circadian clock genes, creating a time window for the utilization of RSG in chronotherapy. Although both PAL and TG exhibit pro-inflammatory properties in macrophages, we believe that PAL does not regulate the release of TNF through the clock system, but rather through alternative pathways, such as cell apoptosis [50]. Consequently, the exogenous addition of PAL may stimulate the self-defensive system of macrophages and lead to increased PAL efflux (Fig. 7 a). Nevertheless, further research will be necessary to elucidate these mechanisms comprehensively in the future.

Our study presents several limitations that warrant acknowledgment. Firstly, while we identified a relationship between Bmal1 and TNF-α, we did not conduct an in-depth investigation into how Bmal1 regulates TNF-α expression in macrophages. Nonetheless, existing literature has extensively documented the regulatory role of circadian clock genes on TNF-α through pathways involving NF-κB or MAPK [51–54] [51–54] [51–54]. Secondly, our study revealed that elevated TG levels coincide with increased Bmal1 expression. However, we did not delve into the specific mechanism by which TG regulates circadian clock genes. Given the known influence of a high-fat diet and lipid substances on the circadian clock system, further research is required to comprehensively investigate this aspect. Lastly, we did not employ animal experiments to validate the effectiveness and mechanisms of RSG chronotherapy. However, considering the existing body of research suggesting the therapeutic potential of RSG for cardiovascular diseases and the growing optimization of chronotherapy as a precise treatment approach, we anticipate that animal experiments to investigate RSG

chronotherapy are a logical next step [53]. Nevertheless, we recognize the need for further experimental validation.

5. Conclusions

Our study yields valuable insights into the regulatory dynamics between macrophages and the phenotypic transition of VSMCs. Specifically, the chronotherapeutic application of RSG activates PPARγ, leading to the accumulation of TG within macrophages. Subsequently, these TG facilitate the expression of Bmal1, which, depending on the timing of RSG administration, either advances or delays the phase of TNF-α release rhythm. This phase disparity in TNF-α release rhythm exerts distinct effects on VSMCs' phenotypic transition, primarily mediated through the activation or inactivation of the MAPK signaling pathway (Fig. 8). In summary, our study lays a robust foundation for targeting the circadian clock system as a potential avenue for treating VSMC phenotype switching.

Funding

This work was supported by the 2022 Natural ScienceFoundation of Wannan Medical College (WK2022F11).

Ethics statement

This study was reviewed and approved by the Ethics Committee of Wannan Medical College, with the approval number (WNMC-AWE-2023332).

Data availability statement

The data that support the findings of this study are openly available in Figshare database and the accession number: https://doi.org/10.6084/m9.figshare.25427722.vl.

CRediT authorship contribution statement

Yu Tian: Writing – original draft, Methodology. **Xuanyu Luan:** Writing – original draft. **Kui Yang:** Writing – review & editing, Supervision.

Declaration of competing interest

The authors declare that they have no known competing financial interests or personal relationships that could have appeared to influence the work reported in this paper.

Appendix A. Supplementary data

Supplementary data to this article can be found online at https://doi.org/10.1016/j.heliyon.2024.e30708.

References

[1] Matthew R. Alexander, Gary K. Owens, Epigenetic control of smooth muscle cell differentiation and phenotypic switching in vascular development and disease, Annu. Rev. Physiol. 74 (2012) 13–40.
[2] Gayathri Viswanathan, et al., Single-cell analysis reveals distinct immune and smooth muscle cell populations that contribute to chronic thromboembolic pulmonary hypertension, Am. J. Respir. Crit. Care Med. 207 (10) (2023) 1358–1375.
[3] Dong Im Cho, et al., ANGPTL4 stabilizes atherosclerotic plaques and modulates the phenotypic transition of vascular smooth muscle cells through KLF4 downregulation, Exp. Mol. Med. 55 (2) (2023) 426–442.
[4] Nikolaos T. Skenteris, et al., Osteomodulin attenuates smooth muscle cell osteogenic transition in vascular calcification, Clin. Transl. Med. 12 (2) (2022) e682.
[5] Hao-Yue Tang, et al., Vascular smooth muscle cells phenotypic switching in cardiovascular diseases, Cells 11 (24) (2022) 4060.
[6] Guoquan Yin, et al., Crosstalk between macrophages and innate lymphoid cells (ILCs) in diseases, Int. Immunopharm. 110 (2022) 108937.
[7] Federica De Paoli, et al., Macrophage phenotypes and their modulation in atherosclerosis, Circ. J.: official journal of the Japanese Circulation Society 78 (8) (2014) 1775–1781.
[8] Michael Peled, Edward A. Fisher, Dynamic aspects of macrophage polarization during atherosclerosis progression and regression, Front. Immunol. 5 (2014) 579.
[9] Charna Dibner, et al., The mammalian circadian timing system: organization and coordination of central and peripheral clocks, Annu. Rev. Physiol. 72 (2010) 517–549.
[10] Ethan D. Buhr, Joseph S. Takahashi, Molecular components of the Mammalian circadian clock, Handb. Exp. Pharmacol. 217 (2013) 3–27.
[11] James O. Early, et al., Circadian clock protein BMAL1 regulates IL-1β in macrophages via NRF2, Proc. Natl. Acad. Sci. U.S.A. 115 (36) (2018) E8460–E8468, https://doi.org/10.1073/pnas.1800431115.
[12] Arisa Yaekura, et al., Chronotherapy targeting cytokine secretion attenuates collagen-induced arthritis in mice, Int. Immunopharm. 84 (2020) 106549.
[13] Jerzy Kotlinowski, Alicja Jozkowicz, PPAR gamma and angiogenesis: endothelial cells perspective, J. Diabetes Res. 2016 (2016) 8492353.
[14] Ningning Wang, et al., Vascular PPARgamma controls circadian variation in blood pressure and heart rate through Bmal1, Cell Metabol. 8 (6) (2008) 482–491.
[15] Wan Jin, et al., *Pers* reverse angiotensin II -induced vascular smooth muscle cell proliferation by targeting *cyclin E* expression via inhibition of the MAPK signaling pathway, Chronobiol. Int. 40 (7) (2023) 903–917.
[16] Andy W.C. Man, et al., Circadian rhythm: potential therapeutic target for atherosclerosis and thrombosis, Int. J. Mol. Sci. 22 (2) (2021) 676.

[17] Shigehiro Ohdo, et al., Chronopharmacological strategies focused on chrono-drug discovery, Pharmacol. Ther. 202 (2019) 72–90.
[18] Long Tao, et al., Light therapy in non-seasonal depression: an update meta-analysis, Psychiatr. Res. 291 (2020) 113247.
[19] Ramón C. Hermida, et al., Chronotherapy with conventional blood pressure medications improves management of hypertension and reduces cardiovascular and stroke risks, Hypertens. Res.: official journal of the Japanese Society of Hypertension 39 (5) (2016) 277–292.
[20] Jiajie Luan, et al., Valsartan-mediated chronotherapy in spontaneously hypertensive rats via targeting clock gene expression in vascular smooth muscle cells, Arch. Physiol. Biochem. 128 (2) (2022) 490–500.
[21] Feng Li, et al., BMAL1 regulates *Propionibacterium acnes*-induced skin inflammation via REV-ERBα in mice, Int. J. Biol. Sci. 18 (6) (21 Mar. 2022) 2597–2608.
[22] Jun Ma, et al., The combined effect of serum cystatin C and dyslipidemia on hypertension in a large health check-up population in China, Clin. Exp. Hypertens. 41 (8) (2019) 702–707.
[23] Y. Kui, et al., Combination of valsartan and melatonin to treat non-dipping hypertension rats via circadian clock system, Int. J. Pharmacol. 17 (7) (2021) 442–454.
[24] Mengru Xie, et al., BMAL1-Downregulation aggravates *porphyromonas gingivalis*-induced atherosclerosis by encouraging oxidative stress, Circ. Res. 126 (6) (2020) e15–e29.
[25] Zhen Sun, et al., Circadian rhythm disorders elevate macrophages cytokines release and promote multiple tissues/organs dysfunction in mice, Physiol. Behav. 249 (2022) 113772.
[26] Changpo Lin, et al., Clock gene Bmal1 disruption in vascular smooth muscle cells worsens carotid atherosclerotic lesions, Arterioscler. Thromb. Vasc. Biol. 42 (5) (2022) 565–579.
[27] Chen Wang, et al., Circadian gene CLOCK accelerates atherosclerosis by promoting endothelial autophagy, Biotechnol. Genet. Eng. Rev. (22 Mar. 2023) 1–16.
[28] Ryan K. Alexander, et al., Bmal1 integrates mitochondrial metabolism and macrophage activation, Elife 9 (12 May) (2020) e54090.
[29] Gareth B. Kitchen, et al., The clock gene *Bmal1* inhibits macrophage motility, phagocytosis, and impairs defense against pneumonia, Proc. Natl. Acad. Sci. U.S.A. 117 (3) (2020) 1543–1551.
[30] Shogo Sato, et al., A circadian clock gene, Rev-erbα, modulates the inflammatory function of macrophages through the negative regulation of Ccl2 expression, J. Immunol. 192 (1) (2014) 407–417.
[31] Shan Chen, et al., A pro- and anti-inflammatory Axis modulates the macrophage circadian clock, Front. Immunol. 11 (2020) 867.
[32] Vanessa Leone, et al., Effects of diurnal variation of gut microbes and high-fat feeding on host circadian clock function and metabolism, Cell Host Microbe 17 (5) (2015) 681–689.
[33] Jian Hao, et al., Qing'e Pill Inhibits Osteoblast Ferroptosis via ATM Serine/Threonine Kinase (ATM) and the PI3K/AKT Pathway in Primary Osteoporosis, Front. Pharmacol. 13 (5 Jul) (2022) 902102.
[34] Shuping Sun, et al., Anti-inflammatory activity of the water extract of Chloranthus serratus roots in LPS-stimulated RAW264.7 cells mediated by the Nrf2/HO-1, MAPK and NF-κB signaling pathways, J. Ethnopharmacol. 271 (2021) 113880.
[35] Yudan Zheng, et al., Antimony-induced astrocyte activation via mitogen-activated protein kinase activation-dependent CREB phosphorylation, Toxicology letters 352 (2021) 9–16.
[36] Weiya Pei, et al., LncRNA AK085865 depletion ameliorates asthmatic airway inflammation by modulating macrophage polarization, Int. Immunopharm. 83 (2020) 106450.
[37] Yi-Jin Wu, et al., α-Mangostin inhibited M1 polarization of macrophages/monocytes in antigen-induced arthritis mice by up-regulating silent information regulator 1 and peroxisome proliferators-activated receptor γ simultaneously, Drug Des. Dev. Ther. 17 (23 Feb. 2023) 563–577.
[38] Yu Wang, et al., Light- and temperature-entrainable circadian clock in soybean development, Plant Cell Environ. 43 (3) (2020) 637–648.
[39] Douglas J. Kojetin, P Burris Thomas, REV-ERB and ROR nuclear receptors as drug targets, Nat. Rev. Drug Discov. 13 (3) (2014) 197–216.
[40] Marine Adlanmerini, A Lazar Mitchell, The REV-ERB nuclear receptors: timekeepers for the core clock period and metabolism, Endocrinology 164 (6) (2023) bqad069.
[41] Huiling Hong, et al., REV-ERBα agonist SR9009 suppresses IL-1β production in macrophages through BMAL1-dependent inhibition of inflammasome, Biochem. Pharmacol. 192 (2021) 114701.
[42] Weiliang Jiang, et al., The MiR-135b-BMAL1-YY1 loop disturbs pancreatic clockwork to promote tumourigenesis and chemoresistance, Cell Death Dis. 9 (2 149. 2 Feb. 2018).
[43] Liangwei Mei, et al., Hsa-let-7f-1-3p targeting the circadian gene Bmal1 mediates intervertebral disc degeneration by regulating autophagy, Pharmacol. Res. 186 (2022) 106537.
[44] Yi Yang, et al., Down-regulation of BMAL1 by MiR-494-3p promotes hepatocellular carcinoma growth and metastasis by increasing GPAM-mediated lipid biosynthesis, Int. J. Biol. Sci. 18 (16) (2022) 6129–6144.
[45] Fangjun Yu, et al., Deficiency of intestinal Bmal1 prevents obesity induced by high-fat feeding, Nat. Commun. 12 (1) (7 Sep. 2021) 5323.
[46] Akira Kohsaka, et al., High-fat diet disrupts behavioral and molecular circadian rhythms in mice, Cell Metabol. 6 (5) (2007) 414–421.
[47] Laura Sardon Puig, et al., Influence of obesity, weight loss, and free fatty acids on skeletal muscle clock gene expression, Am. J. Physiol. Endocrinol. Metabol. 318 (1) (2020) E1–E10.
[48] Erika K. Tse, et al., Role of the saturated fatty acid palmitate in the interconnected hypothalamic control of energy homeostasis and biological rhythms, Am. J. Physiol. Endocrinol. Metabol. 315 (2) (2018) E133–E140.
[49] Biqing Wang, et al., Disruption of USP9X in macrophages promotes foam cell formation and atherosclerosis, J. Clin. Invest. 132 (10) (2022) e154217.
[50] Liang Tao, et al., RIP1 kinase activity promotes steatohepatitis through mediating cell death and inflammation in macrophages, Cell Death Differ. 28 (4) (2021) 1418–1433.
[51] Bing Li, et al., The circadian clock regulator Bmal1 affects traumatic brain injury in rats through the p38 MAPK signalling pathway, Brain Res. Bull. 178 (2022) 17–28.
[52] Alexandre Abilio S. Teixeira, et al., Doxorubicin modulated clock genes and cytokines in macrophages extracted from tumor-bearing mice, Cancer Biol. Ther. 21 (4) (2020) 344–353.
[53] Sanjay Kaul, A Diamond George, Rosiglitazone and cardiovascular risk, Curr. Atherosclerosis Rep. 10 (5) (2008) 398–404.
[54] Bruce M. Psaty, D Furberg Curt, Rosiglitazone and cardiovascular risk, N. Engl. J. Med. 356 (24) (2007) 2522–2524.